RSC Advances

ROYAL SOCIETY OF CHEMISTRY

www.rsc.org/advances

Graphical Abstract

DFT Studies on the Mechanism of Veratryl Alcohol Oxidation Catalyzed by Cu-phen(phen=1,10-phenanthroline) Complexes

Lisha Ma,[a] Qiancheng Zhang,[a] Lin Cheng,[*a] Zhijian Wu[*b], Jucai Yang,[a]

Synopsis to the table of contents:

Density functional theory (DFT) calculations have been performed to investigate the catalytic mechanism for the oxidation of veratryl alcohol to veratraldehyde by Cu-phen(phen=1,10-phenanthroline) catalyst. On the basis of the analysis of overall mechanism, the most favorable mechanism has been predicted and we hope the obtained results could provide useful insights for the reaction process and are useful for future design of more efficient catalysts.

The graphic:

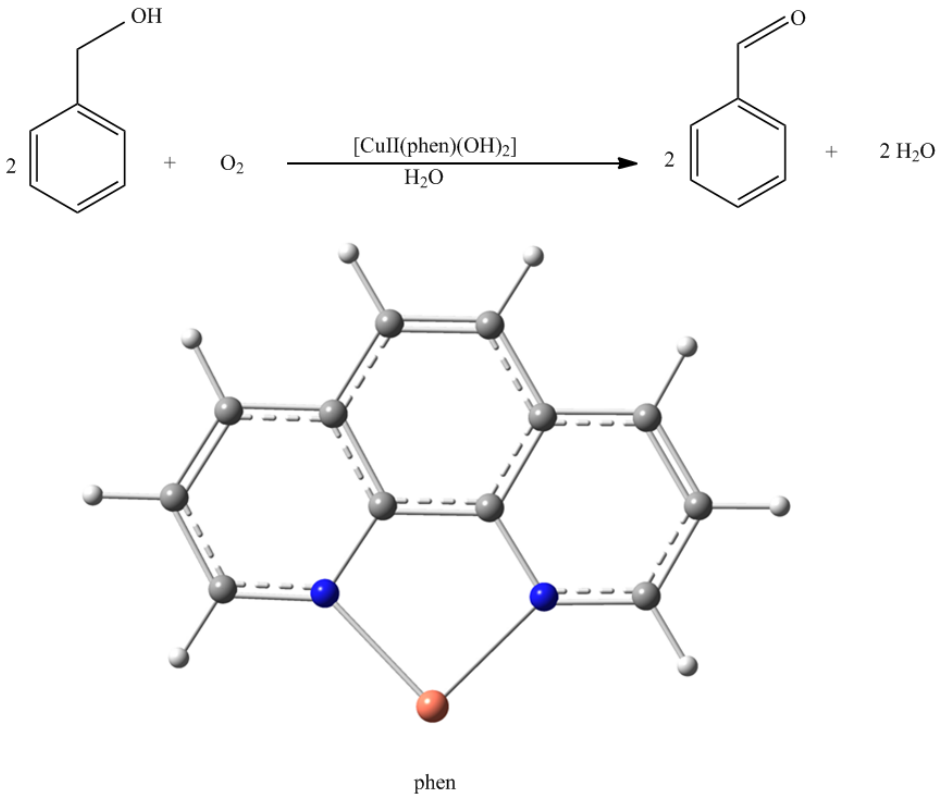

DFT Studies on the Mechanism of Veratryl Alcohol Oxidation Catalyzed by Cu-phen (phen=1,10-phenanthroline) Complexes

Lisha Ma,[a] Qiancheng Zhang,[a] Lin Cheng,*[a] Zhijian Wu,*[b] Jucai Yang,[a]

DOI: 10.1039/b000000x

Density functional theory (DFT) calculations have been performed to investigate the catalytic mechanism for the oxidation of veratryl alcohol to veratraldehyde by Cu phen (phen=1,10-phenanthroline) catalyst. The catalytic cycle consists alcohol oxidation and O_2 reduction. For the alcohol oxidation, both mononuclear mechanism (path A) and binuclear mechanism (path B) are proposed. Our calculations show that path B is preferred over path A. Namely, for the Cu-phen (phen=1,10-phenanthroline) catalytic system, the mechanism is the binuclear mechanism, in consistent with the experimental suggestion. For the O_2 reduction, two possible paths are proposed as well, which are (1) "path I" in which Cu^I is oxidized by O_2 via a binuclear mechanism, and (2) "path II" in which Cu^I is oxidized by O_2 via a mononuclear mechanism. According to our calculations, path I is favored both in thermodynamics and kinetics.

1 Introduction

Selective oxidation of alcohols to the corresponding aldehydes and ketones plays an important role in the organic synthesis of large-scale chemical industry. [1] It is known that traditional alcohol oxidation employs stoichiometric amounts of oxidizing reagents. Unfortunately, most of them suffer from the forcing conditions and toxic stoichiometric oxidations.[2] Thus, the development of catalytic aerobic oxidation is necessary. Galactose oxidase (GOase) is a mononuclear copper enzyme that converts a variety of primary alcohols to aldehydes in the presence of oxygen.[3] A great number of active catalysts have been synthesized as the functional models of GOase. In this aspect, the most studied systems are catalytic system Cu(II)-TEMPO (TEMPO=2,2,6,6-tetramethyl-piperidinyloxyl).[4-13] For instance, Semmelhack and co-workers reported an aerobic oxidation of benzylic and allylic alcohols with 10% CuCl/TEMPO in DMF (N,N-dimethyllformamide) as the solvent.[9] Sheldon and coworkers reported a series of CuII/diimine-TEMPO systems.[4,7] At room temperature and under atmospheric air, CuII/diimine-TEMPO systems could oxidize benzyl alcohol to benzaldehyde. However, the alcohol oxidation has to carry out by the high catalyst loadings (5 mol%), with tBuOK as the catalytic base and CH_3CN/H_2O as the mixture solvent. Reedijk and coworkers studied an efficient catalytic system TEMPO/Cu-pyrazole.[10] However, this catalytic system also requires organic solvent and basic co-catalyst. Recently, S. S. Stahl and coworkers reported a series (bpy)Cu^I/TEMPO systems.[11-13] Among the aerobic alcohol oxidation reported to date, CH_3CN has been used as solvent. Since this will cause safety issues associated with the flammability of organic solvent and oxygen mixtures,[14] it would

be highly desirable to use water as the reaction solvent. In this sense, Cu^{II}/1,10-phenanthroline catalytic system for aerobic oxidation of veratryl alcohol using water as the only solvent would be interesting.[15] In experimental study, binuclear reaction mechanism has been proposed,[15] similar to the mechanism in GOase functional complex.[16] However, previous studies[17,18] suggest that besides binuclear reaction mechanism, the mononuclear reaction mechanism is also possible for Cu/bipy-TEMPO systems.[4,7,19] Therefore, based on the density functional theory, the reaction mechanism of aerobic veratryl alcohol oxidation catalyzed by Cu^{II}/1,10-phenanthroline has been studied by considering both mechanisms. We hope the obtained results could provide useful insights for the reaction process and are useful for future design of more efficient catalysts.

Computational methods

The calculations were performed by use of Gaussian 03 suite of programs.[20] In the model reaction, the substrate veratryl alcohol is simplified to benzyl alcohol. Geometry optimizations and thermal corrections are performed with B3LYP[21] functional and the standard 6-31G(d) basis set. Relative free energies are obtained by single point calculations at B3LYP/6-311+G(d,p) and by including thermal corrections to free energies at B3LYP/6-31G(d). This includes entropy contributions by taking into account the vibrational, rotational and translational motions of the species at 298.15 K. Open-shell calculations for anti-ferromagnetic coupled singlet state usually result in a spin contamination. Therefore, an energy correction was estimated from the Heisenberg spin-Hamiltonian formalism.[22] Similar energy correction approach was used in the previous studies.[23,24] The spin densities (ρ) were generated by Mulliken population analysis with a larger basis set (6-311+G(d,p)). The intrinsic reaction coordinate (IRC) approach was used to confirm that the transition state connects the two relevant minima.[25] The solvent effect on the potential energy surface was investigated by single-point calculations at the B3LYP/6-311+G(d,p) level with the conductor-like polarized continuum solvent model (CPCM)[26] using water (ε = 78.39) as solvent. All the energies values are obtained at solvent (and in kcal/mol).

Result and Discussion

The catalytic cycle of Cu-phen system consists of two parts, namely, alcohol oxidation and O_2 reduction (Scheme 1). The corresponding cartesian coordinates of all structures provided in the Electronic Supplementary Information (ESI) . For the alcohol oxidation, two paths were proposed, i.e., mononuclear mechanism (path A) and binuclear mechanism (path B). For the O_2 reduction, two paths were proposed as well, i.e., path I and path II. The corresponding energy profiles and the optimized geometries for the alcohol oxidation and O_2 reduction are given in Fig. 1, Fig. 2 and Fig.3, respectively.

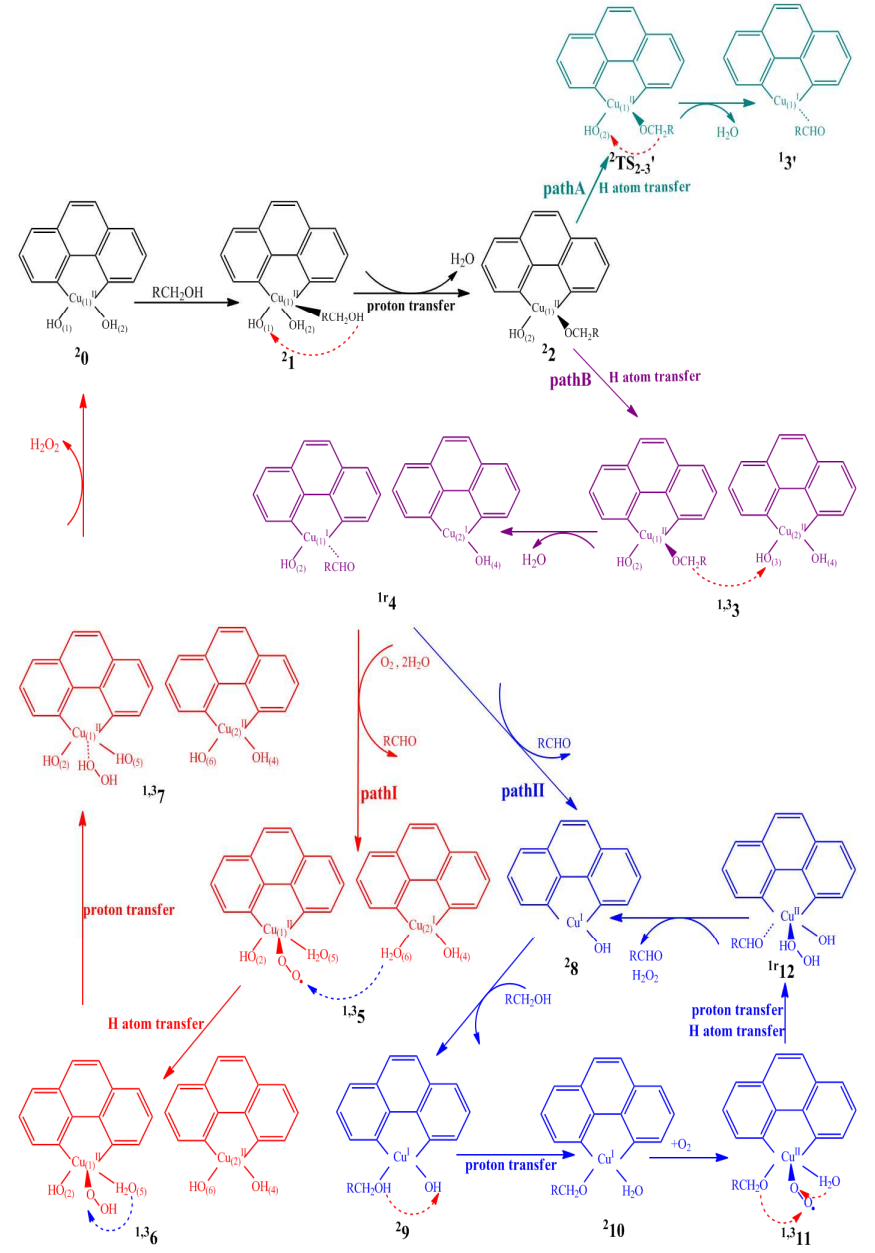

Scheme 1 Proposed catalytic mechanisms of the title complexes. The green, purple colors represent path A and path B. The red, blue colours represent path I and path II, respectively. (The superscript "r" represents closed shell singlet state.)

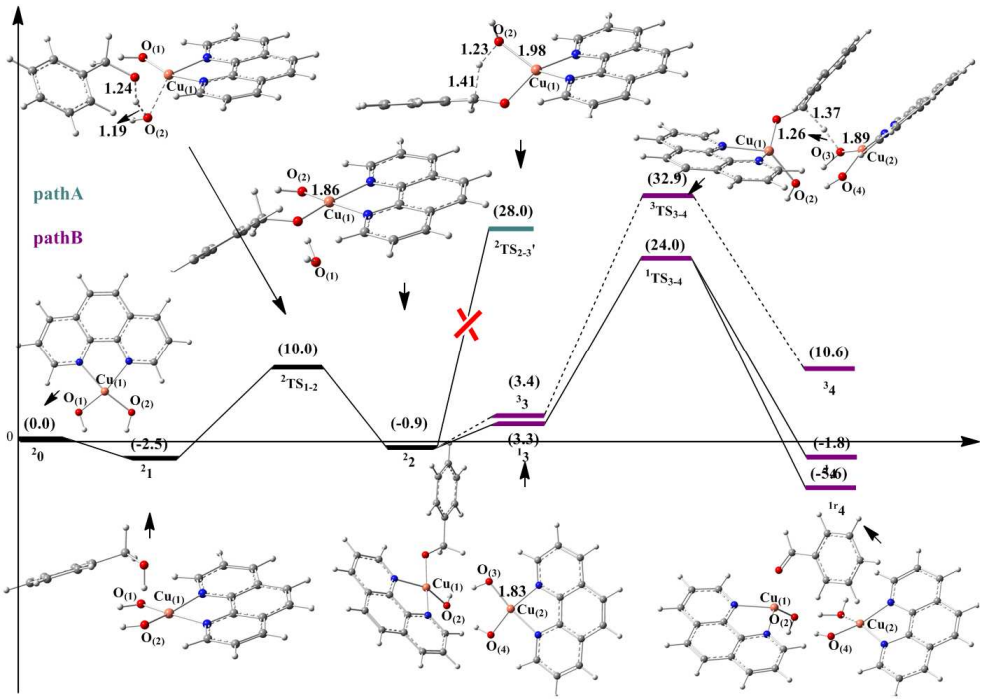

Fig. 1 The optimized geometries and energy profile of the reactant, intermediates, transition states and product for substrate oxidation in path A and path B. The dashed line represents triplet spin state; solid line represents open-shell state. The energy values are in kcal/mol and bond lengths are in Å. (The superscript "r" represents closed shell singlet state.The orange ,red, white balls represent Cu atoms,O atoms and H atoms, respectively. The blue, gray balls represent N atoms and C atoms, respectively.)

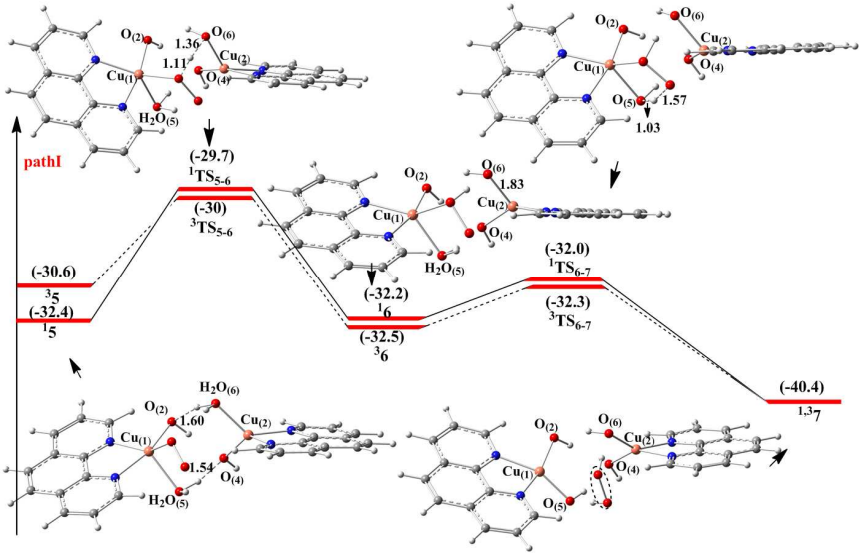

Fig. 2 The optimized geometries and energy profile of the reactant, intermediates, transition states and product for O_2 reduction in path I. The dashed line represents triplet spin state; solid

line represents singlet state. The energy values are in kcal/mol and bond lengths are in Å (The orange ,red, white balls represent Cu atoms,O atoms and H atoms, respectively. The blue, gray balls represent N atoms and C atoms, respectively.)

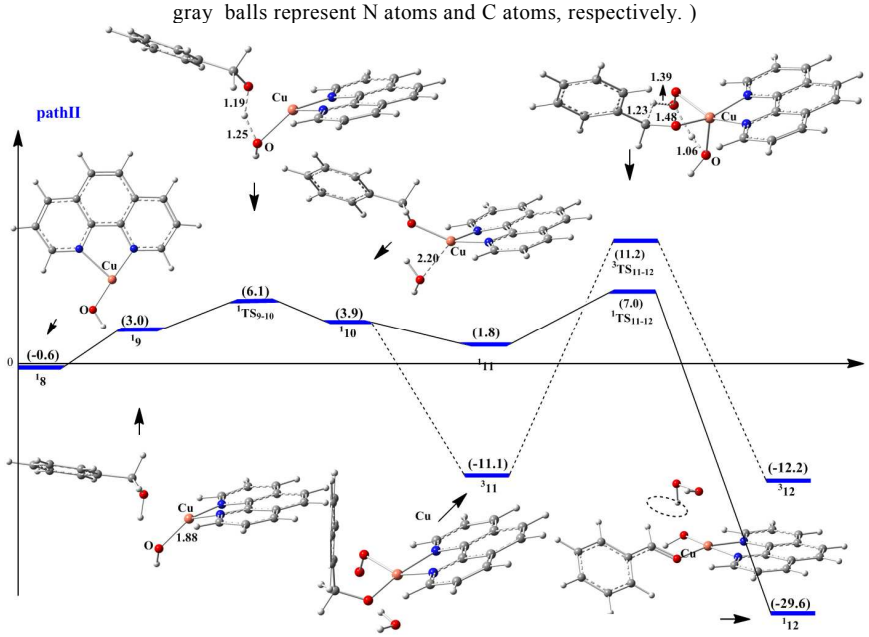

Fig. 3 The optimized geometries and energy profile of the reactant, intermediates, transition states and product for O_2 reduction in path II. The dashed line represents triplet spin state; solid line represents singlet state. The energy values are in kcal/mol and bond lengths are in Å.(The orange ,red, white balls represent Cu atoms,O atoms and H atoms, respectively. The blue, gray balls represent N atoms and C atoms, respectively.)

3.1 Substrate oxidation

3.1.1 proton transfer(0→1→2)

Based on the experimental study, the [Cu^{II}(phen)$(OH)_2$] (denoted as 0 in Fig. 1) is considered as the starting structure for the catalytic reaction. The substrate benzyl alcohol initially coordinates to the Cu^{II} center to give ^{2}1, followed by proton transfer from the substrate benzyl alcohol to the -$O_{(1)}$H group via the transition $^2TS_{1\text{-}2}$ to form ^{2}2. The energy barrier (^{2}1→$^2TS_{1\text{–}2}$) for the proton transfer is 12.5 kcal/mol.

3.1.2 Hydrogen-Abstraction Step(2→3→4)

After the formation of ^{2}2, two paths (path A and path B) are explored. In path B, the precursor (^{2}0) coordinates to 2 forming 3 (with the binuclear center), followed by the H atom moving to the $O_{(3)}$H group to generate 4. For 3, two spin states were considered (singlet state ^{1}3 and triplet state ^{3}3). It is found that ^{1}3 is only 0.1 kcal/mol lower than ^{3}3, indicating that both states are competitive. Consequently, two-state reactivity (TSR) has to be taken into account. The TSR is encountered in many reactions in the organometallic chemistry.[27]As seen in Fig. 1, the open shell singlet state is the ground state in the process 3→4. In this process, the H atom abstraction occurs via $^1TS_{3\text{-}4}$ with the energy barrier of 21.7 kcal/mol with respect to ^{1}3 (24.9 kcal/mol relative to ^{2}2)Thus, the H atom abstraction step is favored and is the rate-determining step. In addition, all of the experimental observations, in the absence of oxygen, only a small percentage (4%) of aldehyde is detected at 80□. In these conditions, the Cu/aldehyde ratio is 2.5 indicating that binuclear reaction

mechanism is favored. While in path A, $^{2}2\rightarrow{}^{1}3$', the H atom moves to the $O_{(2)}H$ group giving H_2O and PhCHO. The calculated energy barrier for the H atom abstraction is 28.9 kcal/mol ($^{2}2\rightarrow{}^{1}TS_{2\text{-}3}$'). During this process, the separation of the OH group from C–H bond is 3.01Å. In $^{1}TS_{2\text{-}3}$', C…H bond distance (bond tends to be broken) is 1.41 Å, while 1.22 Å for O…H (bond tends to be formed). Thus, H atom abstraction results in a "late" transition state. Concluding from both the experimental phenomenon and from the calculated energetics analysis that the results of the pathB is favored.Therefore,in the following, only reactions following path B is discussed.

For $^{1}3$, the positive spin density of ρ = 0.59 on $Cu_{(1)}$, ρ= 0.13 on $phen_{(1)}$, ρ= 0.11 on $O_{(2)}H$, and ρ= 0.13 on the substrate benzyl alcohol are accompanied by a spin density of opposite sign of ρ= -0.56 on $Cu_{(2)}$, ρ= -0.13 on $phen_{(2)}$, ρ= -0.15 on $O_{(3)}H$, and ρ= -0.14 on $O_{(4)}H$. According to the spin density distribution, the complex $^{1}3$ possesses{$[Cu_{(1)}{}^{II}(phen)_{(1)}(O_{(2)}H)(OCH_2Ph)][Cu_{(2)}{}^{II}(phen)_{(2)}(O_{(3)}H)(O_{(4)}H)]$}character. For the product of the H atom abstraction ($^{1r}4$), all the spin densities of the atoms in $^{1r}4$ are zero. $^{1r}4$ is best formulated as {$[Cu_{(1)}{}^{I}(phen)_{(1)}(O_{(2)}H)(OCHPh)][Cu_{(2)}{}^{I}(phen)_{(2)}(O_{(4)}H)]$}. In comparison with $^{1}3$ and $^{1}4$, the above change indicates that the oxidation state of Cu for both $Cu_{(1)}$ and $Cu_{(2)}$ center is reduced from Cu^{II} to Cu^{I}, accompanied by the formation of H_2O and the product PhCHO, which is consistent with the experimental observation.

To further investigate the H atom abstraction, the electron transfer process during $^{1}3\rightarrow{}^{1}TS_{3\text{-}4}$ is discussed. In $^{1}TS_{3\text{-}4}$, the spin density on the $Cu_{(2)}$ center is -0.56, indicating that $Cu_{(2)}$ center is in the Cu^{II} oxidation state. This means that the homolytic cleavage of the $Cu_{(2)}$-$O_{(3)}H$ bond does not occur in $^{1}TS_{3\text{-}4}$. This conclusion could be supported by the $Cu_{(2)}$-$O_{(3)}H$ bond length change ($^{1}3\rightarrow{}^{1}TS_{3\text{-}4}$: 1.83 Å→1.89Å). The bond length change for the similar homolytic cleavage of the Cu-OH bond should be about 0.26 Å.[18] Therefore, the homolytic cleavage of the $Cu_{(2)}$-$O_{(3)}H$ bond did not happen in $^{1}TS_{3\text{-}4}$. Namely, the spin density located on $O_{(3)}H$ should not be affected by the $Cu_{(2)}$-$O_{(3)}H$ bond in $^{1}TS_{3\text{-}4}$. However, for the $O_{(3)}H$ group, the spin density changes from -0.15 to -0.05 in the process of $^{1}3\rightarrow{}^{1}TS_{3\text{-}4}$, indicating that a very small fraction of α-spin electron has been migrated to the $O_{(3)}H$ species. This fraction of the α-spin electron comes from the homolytic cleavage of C_α-H bond of $^{\cdot}OCH_2Ph$. The corresponding β-spin electron generating from homolytic cleavage of C_α-H bond migrates to the substrate, which should result in the decrease of the α-spin density on the substrate. However, it is interesting to mention that the α-spin density on the substrate increases from +0.16 to +0.55, indicating some α-spin densities migrate to the substrate. In addition, the spin density on $Cu_{(1)}$ center decreases from +0.59 to +0.3 ($^{1}3\rightarrow{}^{1}TS_{3\text{-}4}$), indicating that a small fraction of β-spin electron transferring to the $Cu_{(1)}$ center. The α-spin densities migrating to the substrate and the β-spin electron migrating to the $Cu_{(1)}$ center could trace to a fraction of the homolytic cleavage of the $Cu_{(1)}$-OCHPh bond. This could give a fraction of β-spin electron to the $Cu_{(1)}$ atom and α-spin electron to the substrate radical, which results in the decrease of the α-spin density on $Cu_{(1)}$ center (+0.59→+0.3), coupled with the increase of the α-spin density on OCHPh (+0.13→+0.55). In a word, in the process of $^{1}3\rightarrow{}^{1}TS_{3\text{-}4}$, two bonds were partially homolytic cleavage (partially homolytic cleavage of $Cu_{(1)}$-OCHPh bond and minor homolytic cleavage of the C_α–H bond of the $^{\cdot}OCH_2Ph$ group). This conclusion is further supported by the molecular orbitals for $^{1}3\rightarrow{}^{1}TS_{3\text{-}4}$ (Scheme 2). In the process of $^{1}3\rightarrow{}^{1}TS_{3\text{-}4}$, the increase of a small fraction of the α-spin electron on substrate and

a new small fraction of the β-spin electron distributed on $Cu_{(1)}$ indicates the partial homolytic cleavage of the $Cu_{(1)}$-OCHPh bond. Moreover, a small fraction of the α-spin electron on $O_{(3)}H$ and a new small fraction of the β-spin electron located on substrate implies the partial homolytic cleavage of the C_α–H bond of the $^{\cdot}OCH_2Ph$ group. Thus, only $Cu_{(1)}$-OCHPh bond and C_α–H bond are partially homolytic cleavage in the process of ^{1}3→^{1}TS$_{3\text{-}4}$.

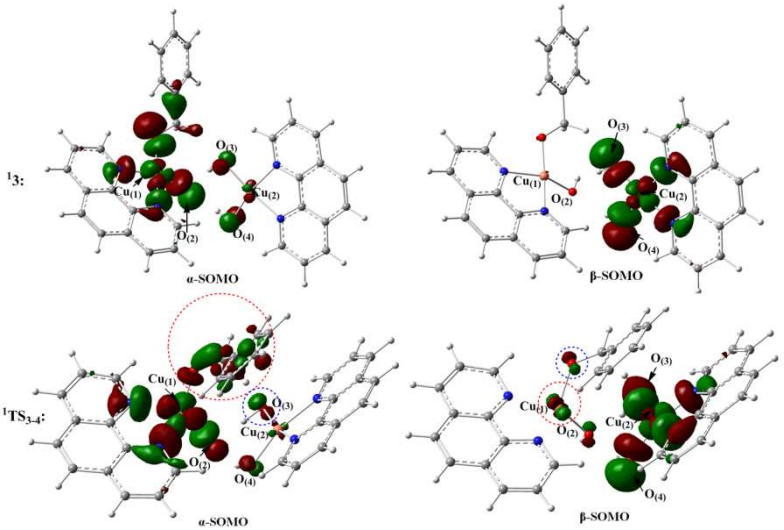

Scheme 2. Molecular orbitals isosurface for ^{1}3 and ^{1}TS$_{3-4}$. SOMO indicates singly occupied molecular orbital. The red, blue colors represent the occupied molecular orbital for the homolytic cleavage of $Cu_{(1)}$-OCHPh bond and C_α-H bond, respectively (contour values = ±0.04).

3.2 O_2 reduction

For the O_2 reduction step, two pathways (path I and path II) are proposed based on the experimental observation (Scheme 1). In path I, O_2 initially replaces the product PhCHO to coordinate to the $Cu_{(1)}$ center in 4 generating 5. Then, after the H atom and a proton transfer steps, the H_2O_2 and PhCHO are formed (6→7). Finally, the release of the H_2O_2 and PhCHO will result in the regeneration of ^{2}0. In contrast, in path II, the H_2O and product PhCHO dissociate before O_2 binding, generating of two units of 8, which is formulated as [Cu^I(phen)(OH)]. Subsequently, another alcohol molecule coordinates to the [Cu^I(phen)(OH)] complex (9→10), followed by the O_2 binding to the Cu^I center to give 11. Then, after the proton and H atom transfer steps, alcohol is converted to aldehyde (11→12). Finally, the release of the H_2O_2 and product PhCHO will result in the regeneration of 8.

3.2.1 Path I

From ^{1r}4, O_2 replaces aldehyde to coordinate to the $Cu_{(1)}$ ion generating ^{1,3}5. Only the end-on binding of oxygen to $Cu_{(1)}$ has been obtained for ^{1,3}5. Since ^{3}5 is 1.8 kcal/mol lower than ^{1}5, two spin states are considered (Fig. 2). As seen in Fig 2, the energies for both two spin states are very close, with the triplet state is a little lower. Therefore, only the triplet state is discussed in the process of 5→7. ^{3}5 is stabilized by two hydrogen bonds [d($O_{(2)}$…$H_2O_{(6)}$) = 1.60 Å and d($O_{(4)}$…$H_2O_{(5)}$) = 1.54 Å). Since the stabilizing effect of the two hydrogen bonds, the ^{1r}4→^{3}5 process is

exothermic by 26.8 kcal/mol. In addition, for $^{3}5$, the calculated spin densities on $Cu_{(1)}$, O_2 species and $Cu_{(2)}$ are 0.61, 1.10 and 0.00, respectively, indicating the $Cu_{(1)}$II-$OO^{\cdot-}$…$Cu_{(2)}$I character. In the process $^{3}5\rightarrow{}^{3}6$, the calculated spin densities on $Cu_{(2)}$ increases from 0 to 0.65, coupled with the spin density on OO·- changing from 1.10 to 0.09. Meanwhile, the OO·- abstract a H atom from $H_2O_{(6)}$ to form OOH- moiety. This implies that the homolytic cleavage of the O-H bond in $H_2O_{(6)}$ is observed. This could result in an β-spin electron transferring to the $O_{(6)}$H group and an α-spin electron to the H atom which migrates to the OO·- species to form OOH- moiety. It is obvious that the β-spin electron located on the $O_{(6)}$H group should be very unstable. Therefore, the $Cu_{(2)}$I offer one electron to couple with the $O_{(6)}$H radical to form the $Cu_{(2)}$II -$O_{(6)}$H bond. This is confirmed by the spin densities on $Cu_{(2)}$ center (increases from 0 to 0.65 in the process of $^{3}5\rightarrow{}^{3}6$) and the bond length change ($^{3}5\rightarrow{}^{3}6$: 2.01→1.83Å). After the H atom transfer step, another proton transfers from $H_2O_{(5)}$ to -OOH moiety, generating H_2O_2. Finally, the release of H_2O_2 could regenerate catalyst 0.

3.2.2 Path II

The generated aldehyde dissociates from $^{1r}4$ forming two units of [Cu^{I}(phen)(OH)] ($^{1}8$). In the process $^{1r}4\rightarrow{}^{1}8$ (Fig.1 and Fig. 3), the reaction is endothermic by 5.0 kcal/mol. It is obvious that the generation of $^{1}8$ (path II) is thermodynamically unfavorable when compared to $^{1}5$ (path I). After the formation of $^{1}8$, the substrate alcohol coordinates to the Cu center giving $^{1}9$, followed by the proton transfer from alcohol to hydroxy group, generating $^{1}10$. The energy barrier for this proton-transfer step ($^{1}9\rightarrow{}^{1}TS_{9-10}$) is 3.1 kcal/mol. In the process of $^{1}9\rightarrow{}^{1}10$, the Cu-O distance increases from 1.88 to 2.20Å, suggesting that the Cu-O bond is fully cleaved, forming the water molecule (H_2O) in $^{1}10$. From $^{1}10$, the triplet O_2 coordinates to the Cu center generating $^{1,3}11$. $^{3}11$ is lower in energy than $^{1}11$ by 12.9 kcal/mol. As seen in Fig. 3, the triplet state cross over to the open-shell singlet surface en route to $^{1}TS_{11-12}$. Although the $^{1}TS_{11-12}$ is 4.2 kcal/mol lower than $^{3}TS_{11-12}$, the reactivity are still be dominated by the triplet state, because of the large energy difference between $^{3}11$ and $^{1}11$ (12.9 kcal/mol). Similar situation was encountered in Shaik's work (case C in that study). [28] The activation energy for $^{3}11\rightarrow{}^{3}12$ is 22.3 kcal/mol.After the migration steps of proton and hydrogen atom, $^{3}12$ is formed. The spin densities for $^{3}12$ implies the [(·OCHPh)Cu^{II}(phen)(OH)(H_2O_2)] character. To form product PhCHO, the [·OCHPh-Cu^{II}] bond has to cleave (generating one α-spin electron and one β-spin electron). Then, the β-spin electron migrates to the ·OCHPh species to form product PhCHO. And the α-spin electron should transfer to Cu^{II} ion. As we know, Cu^{II} ion is in the d^9 character, which could accommodate a β-spin electron. However, the homolytic cleavage of the ·OCHPh-Cu^{II} bond generates an α-spin electron. Therefore, the α-spin electron has to spin-flip to β-spin electron to migrate to Cu^{II} ion, giving rise to the Cu^{I} and to give $^{1r}12$. After the formation of $^{1r}12$, the products benzaldehyde and H_2O_2 are released to regenerate $^{1}8$.

In summary, the $^{1r}4\rightarrow{}^{3}5$ process is exothermic by 26.8 kcal/mol and the energy barrier for path I (about 3 kcal/mol) is observed (22.3 kcal/mol in path II). Therefore, for the O_2 oxidation reaction, path I is the preferred pathway.

Calculations of the veratryl alcohol Oxidation

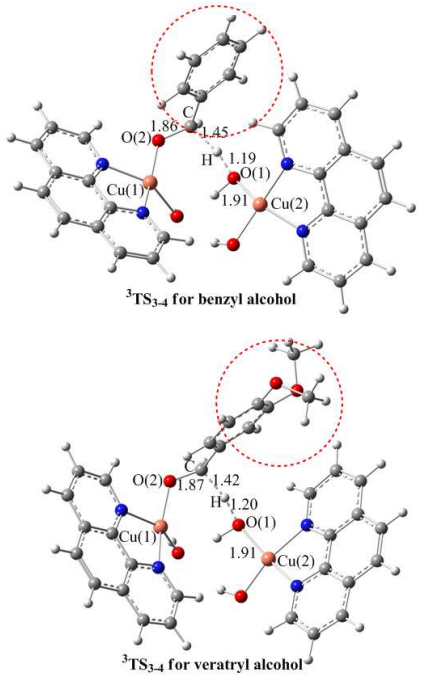

Fig. 4 The optimized geometries for the transition states in both substrate benzyl alcohol and veratryl alcohol. The bond lengths are in Å.(The orange ,red, white balls represent Cu atoms,O atoms and H atoms, respectively. The blue, gray balls represent N atoms and C atoms, respectively.)

Because the substrate veratryl alcohol was simplified to benzyl alcohol, which could introduce extra errors in the activation barriers, we performed calculations on benzyl alcohol as the substrate for the critical reaction steps in both path A and path B.On the basis of our calculations, the geometry structures (Fig.4) and the energy barriers for the critical reaction steps in path A and path B are quite similar for veratryl alcohol and benzyl alcohol. As an example, the energy barriers for the H abstraction step (rate-determining step in path B) for veratryl alcohol and benzyl alcohol are within 0.5kcal/mol. And the critical bond lengths are shown in the following table1. As seen in the table below, the differences are within 0.03Å. This implies that benzyl alcohol represents a good trade-off between accuracy and computational cost in exploring the whole energetic profile.

Table1.The bond lengths for the he transition states in both substrate benzyl alcohol and veratryl alcohol

model	O(1)...H	C...H	Cu(1)-O(2)	Cu(2)-O(1)
benzyl alcohol	1.19Å	1.45Å	1.86Å	1.91Å
veratryl alcohol	1.20Å	1.42Å	1.87Å	1.91Å

wB97XD

wB97XD is the latest functional from Head-Gordon and coworkers, which includes empirical dispersion.[30] Therefore, we chose the wB97XD functional as the alternative functional to recalculate the critical reaction steps in both path A and

path B. For the open shell singlet state, the large spin contamination (S2>3) for wB97XD was observed, implying wB97XD is not suitable to describe the open shell singlet. But for the triplet state, wB97XD functional gives the very similar geometry structures and the energy barriers compared to B3LYP. In addition, B3LYP has been tested extensively in many studies of molecular structures and is a suitable functional for describing the open shell singlet.[29] Thus, we suppose the B3LYP functional give reliable results in this catalytic system.

Conclusions

The catalytic mechanism for the oxidation of veratryl alcohol to veratraldehyde by Cu-phen (phen=1,10-phenanthroline) catalyst have been performed by use of density functional method. The catalytic cycle consists of two parts, namely, alcohol oxidation and O_2 reduction. For the alcohol oxidation, two mechanisms were proposed, i.e., mononuclear mechanism and binuclear mechanism. The calculations show that the H-atom transfer step within the alcohol oxidation is the rate-determining step for both paths. The calculated overall reaction barrier for path A is 28.9 kcal/mol, larger than 24.9 kcal/mol for path B, indicating that path B is favorite. Namely, for the Cu-phen (phen=1,10-phenanthroline) catalytic system, the mechanism is the binuclear mechanism, in agreement with experiment. In addition, for the O_2 reduction, two possible paths are proposed as well (path I and path II). According to our calculations, path I is favored.

References

[a] *Key Laboratory of Industrial Catalysis of the Inner Mongolia Autonomous Region, Inner Mongolia University of Technology, Huhehot 010051, China. Email: lcheng1983@aliyun.com*
[b] *State Key Laboratory of Rare Earth Resource Utilization, Changchun Institute of Applied Chemistry, Chinese Academy of Sciences, Changchun 130022, China. Fax+86 431 85698041, Email: zjwu@ciac.ac.cn*

The authors thank the National Natural Science Foundation of China (NSFC) (Grant No. 21343007) and the Inner Mongolia University of Technology (Grant No. ZD201207) for financial support.

† Electronic Supplementary Information (ESI) available: Table S1 contains the cartesian coordinates of all the structures considered in this work from the B3LYP optimized geometries. See DOI: 10.1039/b000000x/

1 J. M. Hoover, B. L. Ryland and S. S. Stahl, *J. Am. Chem. Soc.*, 2013, **135**, 2357.
2 (a) V.C.H .Wiley, Weinheim. *Ullman´s Encyclopedia of Industrial Chemistry, 6th edn.*, 2002,**12**, 609; (b) Blackie Academic & Proffesional. *Principles of Organic Synthesis, 3rd edn.* London, 1993, 96; (c) R. V. Stevens, K. T. Chapman and H. N. J. Weller, *Org. Chem.*, 1980, **45**, 2030; (d) J. R. J. Holum, *Org. Chem.*, 1961, **26**, 4814; (e) D. G. Lee, U. A. J. Spitzer, *Org. Chem.*, 1970, **35**, 3589; (f) R. J. Highet, W. C. Wildman, *J. Am. Chem. Soc.*, 1955, **77**, 4399; (g) F. M. Menger, C.Lee, *Tetrahedron Lett.*, 1981, **22**, 1655; (h) L. M. Berkowitz, P. N. Rylander, *J. Am. Chem. Soc.*, 1958, **80**, 6682.
3 (a) J. W. Whittaker, H, Sigel, A. Sigel, M. Dekker, *New York*, 1994. **30**, 315; (b) P. F.Knowles, *Bio-inorganic Chemistry*, 1994, **2**, 207.
4 P. Gamez, I.W.C.E. Arends, R.A. Sheldon, J. Reedijk, *Adv. Synth. Catal.*, 2004, **346**, 805.
5 Z. Lu, J.S. Costa, O. Roubeau, I.Mutikainen, U.Turpeinen, S.J.Teat, P. Gamez, J. Reedijk, *Dalton Trans.*, 2008, **27**, 3567.
6 N. Mase, T. Mizumori, Y.Tatemoto, *Chem. Commun.*, 2011, **47**, 2086.
7 P.Gamez, I.W.C.E. Arends, J. Reedijk, R. A.Sheldon, *Chem. Commun.*, 2003, **0**, 2414.
8 J. S. Uber, Y. Vogels, D. van den. Helder, I. Mutikainen, U. Turpeinen, W. T. Fu, O. Roubeau, P.Gamez, J. Reedijk, *Eur. J. Inorg. Chem.*, 2007, **26**, 4197.

9 M. F.Semmelhack, C. R.Schmid, D. A. Cortés, C. S. Chou, *J. Am. Chem. Soc.*, 1984, **106**, 3374.
10 J. S. Uber, Y.Vogels, D. van den.Helder, I. Mutikainen, U.Turpeinen, W. T.Fu, O.Roubeau, P.Gamez, J.Reedijk, *Eur. J. Inorg. Chem*., 2007, **26**, 4197.
11 J. M.Hoover, S. S.Stahl, *J. Am. Chem. Soc*., 2011, **133**, 16901.
12 J. F. Greene, J. M. Hoover, D. S. Mannel, T. W. Root, S. S.Stahl, *Org. Process Res. Dev.*, 2013, **17**, 1247.
13 N. J. Hill, J. M. Hoover, S. S. Stahl, *J. Chem. Educ*., 2013, **90** , 102.
14 A. Sheldon, P.J. Dunn, A.S. Wells, M.T.Williams, *Green Chemistry in the Pharmaceutical Industry*, 2010, pp. 1.
15 H. Korpi, P. J. Figiel, E. Lankinen, P. Ryan, M. Leskel, T. Repo, *Eur. J. Inorg. Chem.*, 2007,**17**, 2465.
16 T. T. K. Esa, M. P. K .Ari, Prof, *Chem. Eur. J*., 2009, **15**, 10901.
17 L.Cheng, J. P.Wang, M. Y. Wang, Z. J. Wu, *Inorg. Chem.*, 2010,**49** ,9392.
18 L.Cheng, J. P. Wang, M. Y. Wang, Z. J. Wu, *Dalton Transaction*, 2010, **39**, 5377.
19 P. J. Figiel, M. Leskel¨a, T. Repo, *Adv. Synth. Catal*. 2007, **349**, 1173.
20 M. J. Frisch, G. W. Trucks, H. B. Schlegel, G. E. Scuseria, M. A. Robb, J. R. Cheeseman, J. A. Montgomery, T. Vreven, K. N. Kudin, J. C. Burant, J. M. Millam, S. S. Iyengar, J. Tomasi, V. Barone, B. Mennucci, M. Cossi, G. Scalmani, N. Rega, G. A. Petersson, H. Nakatsuji, M. Hada, M. Ehara, K. Toyota, R. Fukuda, J. Hasegawa, M. Ishida, T. Nakajima, Y. Honda, O. Kitao, H. M. Nakai, X. Klene, J. E. Li, H. P. Knox, J. B. Hratchian, C. Cross, J. Adamo, Jaramillo, R. Gomperts, R. E. Stratmann, O. Yazyev, A. J. Austin, R. Cammi, C. Pomelli, J. W. Ochterski, P. Y. Ayala, K. Morokuma, G. A. Voth, P. Salvador, J. J. Dannenberg, V. G. Zakrzewski, S. Dapprich, A. D. Daniels, M. C. Strain, O. Farkas, D. K. Malick, A. D. Rabuck, K. Raghavachari, J. B. Foresman, J. V. Ortiz, Q. Cui, A. G. Baboul, J. Clifford, J. Cioslowski, B. B. Stefanov, G. Liu, A. Liashenko, P. Piskorz, I. Komaromi, R. L. Martin, D. J. Fox, T. Keith, M. A. Al-Laham, C. Y. Peng, A. Nanayakkara, M. Challacombe, P. M. W. Gill, B. Johnson, W. Chen, M. W. Wong, C. Gonzalez, J. A. Pople, *Gaussian 03, Gaussian, Inc.: Pittsburgh, PA*, 2003.
21 (a) A. J. Cohen, N. C. Handy,*Mol. Phys*., 2001, **99**, 607; (b) J. Perdew, K. Burke, M. Ernzerhof, *Phys. Rev. Lett*., 1996, **77**, 3865.
22 (a) J. M. Mouesca, J. L. Chen, L. Noodleman, D. Bashford, D. A. Case, *J. Am. Chem. Soc.* 1994, **116**, 11898; (b) L. Noodleman, *J. Chem. Phys.*1981, **74**, 5737; (c) L. Ciofini, C. A. Daul, Coord. *Chem. Rev.*,2003, 238.
23 V. Bachler, G. Olbrich, F. Neese, K. Wieghardt, *Inorg. Chem*., 2002, **41**, 4179.
24 P. E. M. Siegbahn, V. Pelmenschikov, *J. Am. Chem. Soc.*,2006, **128**, 7466.
25 (a) K. Fukui, *Acc. Chem. Res.*,1981, **14**, 363*;* (b) K. Fukui, *J. Phys.Chem.* 1970, **74**, 4161.
26 (a) V. Barone, M. Cossi, *J. Phys. Chem. A.* 1998, **102**, 1995;(b) M. Cossi, G. Scalmani, N. Rega, V. Barone, *J. Comput. Chem*., 2003, **24**, 669.
27 (a) H. Hirao, D. Kumar, W. Thiel, S. Shaik, *J. Am. Chem. Soc.*, 2005, **127**, 13007;(b) S. Cohen, S. Kozuch, C. Hazan, S. Shaik, *J. Am. Chem. Soc.*, 2006, **128**, 11028; (c) E. Derat, S. Shaik, *J. Am. Chem. Soc*., 2006, **128**, 8185; (d) D. Kumar, S. P. de Visser, S. Shaik, *Chem. Eur. J*.,2005, **11**, 2825; (d) M. Guell, J. M. Luis, P. E. M. Siegbahn, M. J. Sola, Biol, *Inorg. Chem*., 2009, **14**, 273.
28 H. Hirao, D.Kumar, L.Que, Jr, S. Shaik, *J. Am. Chem. Soc*., 2006, **128**, 8590.
29 G. Jürgen , K. Elfi , F. Michael, C.Dieter ,*Int. J. Mol. Sci.*, 2002, **3**, 360.
30 M.Yury ,S. Åsmund , O.Giovanni, *Dalton Trans*., 2012, **41**, 5526.